

FIRST CHARACTERIZATION OF THE PHOTON BEAM AT THE EUROPEAN XFEL IN JULY, 2017

V. Balandin, B. Beutner, F. Brinker, W. Decking, M. Dohlus, L. Fröhlich, U. Jastrow, R. Kammering, T. Limberg, D. Noelle, M. Scholz, A. Sorokin, K. Tiedtke, M.V. Yurkov, I. Zagorodnov, DESY, Hamburg, Germany
U. Boesenberg, W. Freund, J. Grünert, A. Koch, N. Kujala, J. Liu, T. Maltezopoulos, M. Messerschmidt, I. Petrov, L. Samoylova, H. Sinn, European XFEL, Germany

Abstract

This report presents the first characterization of the photon beam properties from SASE1 FEL at the European XFEL. Development of the amplification process has been traced from the level of the radiation pulse energy in sub- μJ level (beginning of high gain linear regime) up to mJ level (saturation regime). Experimental method is based on the analysis of single shot photon beam images allowing to derive spatial properties of the FEL radiation mode. An important conclusion is that experimental results demonstrate reasonable agreement with baseline parameters. Developed techniques of the photon beam characterization also provided solid base for identification of the problems and means for improving SASE FEL tuning and operation.

INTRODUCTION

First light from the European XFEL [1] has been detected on May 3rd, 2017 at the photon energy of 1.3 keV and electron beam energy of 6.4 GeV [2]. Start-up phase of the European XFEL included a lot of tasks performed in parallel such as gradual increase of electron energy, tests of hardware, electron beam diagnostics, electron beam formation system, electron beam optics, test and tuning of the undulator, commissioning of photon beam diagnostics and photon beam transport system. Two months after the event of the "first light", operation of all systems improved significantly, and detected radiation pulse energies reached design values in a mJ range. First characterization of the photon beam has been performed in July 2017, a month before an official starting date of user experiments (September 1st, 2017). Energy of the electron beam was 13.5 GeV, bunch charge was 500 pC, radiation wavelength 0.15 nm. Two photon diagnostic systems (FEL imager and X-ray gas monitor (XGM) detector) were available at that time which was sufficient for basic characterization of the radiation. This allowed us to measure the gain curve and trace evolution of the FEL radiation mode along significant part of the amplification regime, from almost beginning of the high gain exponential regime to saturation. Analysis of the FEL radiation modes have shown that in the whole range of the radiation pulse energies (from μJ to mJ level) they are surprisingly close to those predicted ten years ago at the design stage of the project [3]. Measured properties of the electron beam in the accelerator were also in agreement with design parameters [2, 4]. Thus, both results of the electron beam and photon beam measurements provide strong argument in

favor of conclusion that physical parameters of the machine are close to design values.

It turned out that analysis of the spatial properties of FEL radiation modes demonstrated to be a powerful tool for characterization physical parameters of SASE FEL process. As an extension of this experimental method we plan to implement correlations of FEL images with machine parameters which will allow to apply statistical techniques for determination of important parameters of SASE FEL such as gain length, saturation length, coherence time, radiation pulse duration, number of radiation modes in the pulse (longitudinal and transverse), degree of transverse coherence [5–8].

EXPERIMENTAL RESULTS

Measurements have been performed at the North branch of the European XFEL, SASE1 FEL. It is equipped with planar, variable gap undulator with 4 cm period length. It consists of 35 modules, each of 5 meter long. Machine operated at the energy of 13.5 GeV, bunch charge 500 pC, and the radiation wavelength was 0.15 nm. Special efforts have been taken for tuning machine to design parameters of the electron beam [2, 4].

By the time of described experiment only two photon diagnostics tools were in operation: FEL imager and XGM detector [9–13]. FEL imager is equipped with scintillating Ce:YAG screen and a scientific CMOS camera, and is located at a distance of 230 meters downstream the undulator end. XGM detector, located at 185 m behind the undulator, is cal-

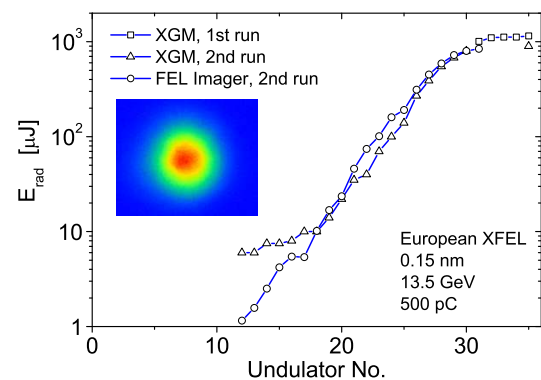


Figure 1: Gain curve of the European XFEL. The inset shows a single photon beam image. Electron energy is 13.5 GeV, bunch charge is 500 pC, radiation wavelength is 0.15 nm.

Content from this work may be used under the terms of the CC BY 3.0 licence (© 2019). Any distribution of this work must maintain attribution to the author(s), title of the work, publisher, and DOI

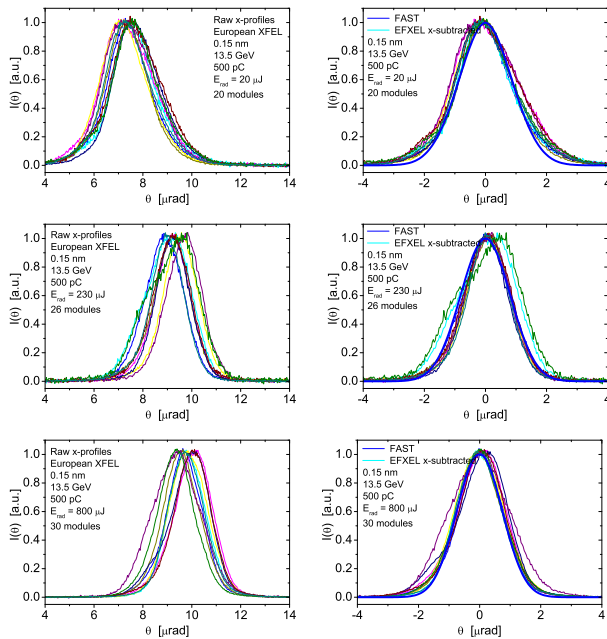


Figure 2: Single shot transverse profiles of the radiation pulses. Thin colored lines show 10 shots of the European XFEL. Left column: raw results. Right column: spatial jitter is subtracted. Bold blue lines on the right hand side are numerical simulations with code FAST [14] for baseline parameters of the electron beam [4]. Average radiation energy in the pulse is 20 μJ (upper row), 230 μJ (middle row), and 800 μJ (bottom row).

ibrated ionization chamber allowing precise measurements of average radiation energy over several pulse trains. XGM is also capable to resolve the shot-to-shot pulse energies at 4.5 MHz repetition rate within trains. However, at pulse energies below 50 μJ the XGM sensitivity is not sufficient to perform absolute measurements, but relative changes can be monitored down to the low level of spontaneous radiation of a single undulator segments.

Machine operated with one bunch per train with macropulse repetition rate 10 Hz, and FEL imager is used for single shot measurements of the photon beam images. Radiation pulse energy is derived by means of calculating the integrated intensity. XGM signal is used for calibration of FEL imager in the trusted dynamic range. A set of solid attenuators is used to keep x-ray flux on a scintillator at a level preventing saturation effects. Also, sCMOS camera is equipped with a set of neutral filters for controlling light intensity coming from scintillator.

Experimental procedure is organized in the following way. We tune SASE FEL to maximum signal at full undulator length (35 undulator modules). Then, keeping fixed all machine parameters, we gradually open undulator sections from the downstream end and record XGM readings and about 200 photon beam images at each step. Plots in Fig. 1 show experimental results for the gain curve. Both results are shown here, XGM and FEL imager. With FEL imager we can detect

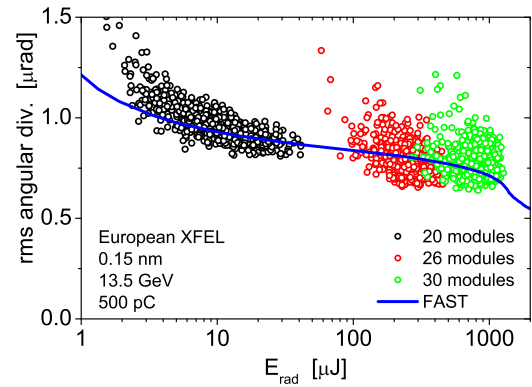


Figure 3: Dependence of the FWHM angular divergence on the radiation pulse energy. Bold blue line shows results of numerical simulations with code FAST [14] for baseline parameters of the electron beam [4]. Full radiation profiles are shown in Fig. 2.

lower, by about an order of magnitude, radiation intensities. The measured gain curve clearly demonstrates a stage of exponential amplification and a saturation regime after 25th module. Measurements at the radiation energies below a fraction of μJ suffer from high noise and background, so amplification process in 1/3rd of the undulator length could not be traced.

Analysis of the photon beam images allows to derive single shot angular distributions of the radiation intensity shown in Fig. 2. Plots in the left column show raw results. Strong pointing jitter takes place which is caused by sporadic electron beam orbit jitter. Subtraction of the spatial jitter allows us to select pure FEL radiation mode (see right column of Fig. 2) and trace its evolution along significant part of the amplification regime, from almost beginning of the high gain exponential regime to saturation (from μJ to mJ level). Bold grey curves on these plots show FEL mode calculated with code FAST [14] for design parameters of the electron beam [3]. Surprisingly good agreement takes place. Angular divergence of the FEL radiation is not a constant value, but it changes in the amplification process. SASE FEL radiation has wider cone at small radiation energies (beginning of the amplification). Then it passes plateau in the high gain exponential regime, and finally shrinks in the nonlinear regime. Signature of this physical behavior is clearly demonstrated when we plot angular divergence as a function of the energy in the radiation pulse. Blue line in Fig. 3 presents simulations with code FAST for baseline parameters, and circles are the results of measurements. Good agreement with predictions for baseline parameters takes place in the whole range. As we already mentioned in the introduction, measured electron parameters were also close to design values. These observations are strong arguments in favor of the statement that physical parameters of the machine are close to design parameters.

Contour plots in Fig. 4 allow to trace SASE FEL parameters in saturation versus emittance and peak current. Base-

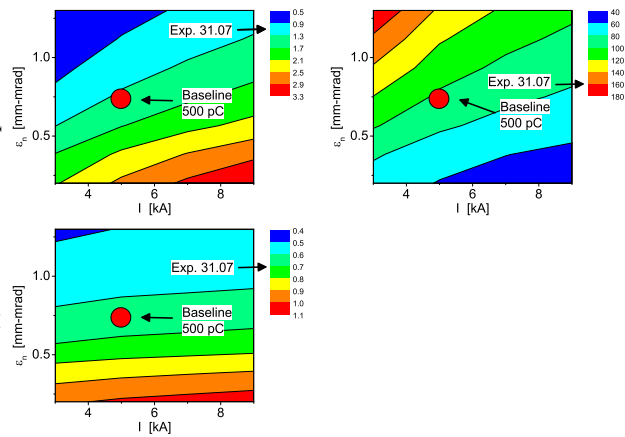


Figure 4: Overview of SASE1 saturation parameters in emittance - peak current parameter space. Calculations are performed with code FAST [14]. Top left: average energy in the radiation pulse (mJ). Top right: saturation length (meters). Bottom left: FWHM angular divergence of the radiation (μrad). Red circles denote operating point with baseline parameters [4]. Arrows directed to scale bars show measured parameters.

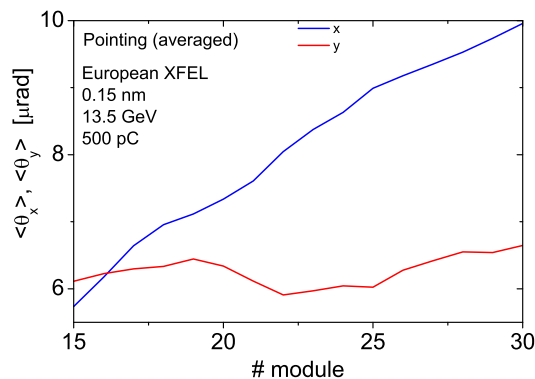


Figure 5: Drift of the photon beam angular pointing along the undulator measured in the experiment.

line parameters are shown as red points on the plots. We see that there is good agreement between measured and design parameters for the values of the radiation pulse, while there is pretty big overhead in the saturation length of about 70%. Note that stability of the machine operation during experiment was far from ideal, and has been disturbed by many sporadic jitters of orbit and beam formation system. In particular, jitter of electron orbit resulted in 30% of the photon beam pointing jitter. Lack of tuning experience also took place, and one of the problems was found during post processing of photon beam images. Figure 5 shows drift of the photon beam angular pointing as function of the undulator length. Since angle is derivative of the transverse displacement of the trajectory, we find that trajectory of the electron beam in the last 15 modules is nearly parabolic with maximum deviation in the end of about 180 μm. Such a strong deviation of the orbit from a straight line results in much

longer saturation length. Also, a problematic region has been identified with large local trajectory kick. So, analysis of the amplification process with screens provides us reliable way for controlling electron beam trajectory imperfections.

DISCUSSION

In this paper we described the first photon beam characterization from the European XFEL. By now similar studies are performed on a regular basis to check physical parameter space and stability of the machine operation. General result of these studies is that physical parameter space of SASE FEL is close to baseline parameters when special efforts are applied for control of the electron beam parameters. Stability of machine operation and quality of tuning improved significantly such that there is only some 20% overhead of the saturation length [2]. However, we still observe that the fluctuation of the radiation pulse energy is mainly driven by jittering accelerators parameters. The nature and source of jittering is under study, and we believe that proper tuning of all systems of the superconducting accelerator will allow reducing fluctuations to the level of fundamental fluctuations as it has been demonstrated at FLASH [5–8].

REFERENCES

- [1] M Altarelli *et al.* (Eds.), Preprint DESY 2006-097, DESY, Hamburg (2007).
- [2] W. Decking *et al.*, “First operation of a MHz-repetition-rate Hard X-Ray Free-Electron Laser driven by a superconducting linear accelerator”, submitted for publication.
- [3] E.A. Schneidmiller and M.V. Yurkov, Preprint DESY 11-152, DESY, Hamburg (2011).
- [4] W. Decking, T. Limberg, XFEL.EU Technical Note 1-22 (2013) XFEL.EU TN-2013-004-01, European XFEL, Hamburg (2013).
- [5] C. Behrens *et al.*, “Constraints on photon pulse duration from longitudinal electron beam diagnostics at a soft x-ray free-electron laser”, *Phys. Rev. ST AB* 15, 030707 (2012). doi : 10.1103/PhysRevSTAB.15.030707
- [6] E. Schneidmiller and M. V. Yurkov, “Application of Statistical Methods for Measurements of the Coherence Properties of the Radiation from SASE FEL”, in *Proc. 7th Int. Particle Accelerator Conf. (IPAC’16)*, Busan, Korea, May 2016, pp. 738–740. doi : 10.18429/JACoW-IPAC2016-MOP0W013
- [7] E.A. Schneidmiller and M.V. Yurkov, CERN Yellow Reports: School Proceedings, Vol. 1, 539-596 (2018). doi : 10.23730/CYRSP-2018-001.539
- [8] O. I. Brovko *et al.*, “Experience With MCP-Based Photon Detector at FLASH2”, presented at the 39th Int. Free Electron Laser Conf. (FEL’19), Hamburg, Germany, Aug. 2019, paper WEP073.
- [9] A. Koch *et al.*, “Design and initial characterisation of X-ray beam diagnostic imagers for the European XFEL”, in *Proc. SPIE* 9512, 95121R-1 (2015). doi : 10.1117/12.2182463
- [10] J. Grünert *et al.*, “X-ray photon diagnostics devices for the European XFEL”, in *Proc. SPIE*, 8504, X-Ray Free-Electron Lasers: Beam Diagnostics, Beamline Instrumentation, and Applications, 85040R (2012). doi : 10.1117/12.929710

- [11] J. Grünert *et al.*, “X-ray photon diagnostics at the European XFEL”, *J. Synchrotron Rad.* 26, 000-000. [XQ5005] (2019). doi:10.1107/S1600577519006611 1107/S1600577519005174
- [12] T. Maltezopoulos *et al.*, “Commissioning of a photoelectron spectrometer for soft X-ray photon diagnostics at the European XFEL”, *J. Synchrotron Rad.* 26, 1045-1051. (2019). doi:10.1107/S1600577519003552
- [13] A.A. Sorokin *et al.*, “An X-ray gas monitor for free-electron lasers”, *J. Synchrotron Rad* 26, 1092-1100 (2019). doi:10.1016/S0168-9002(99)00110-2
- [14] E.L. Saldin, E.A. Schneidmiller and M.V. Yurkov, “FAST: a three-dimensional time-dependent FEL simulation code”, *Nucl. Instrum. and Methods A* 429, 233 (1999). doi:10.1016/S0168-9002(99)00110-2

Content from this work may be used under the terms of the CC BY 3.0 licence (© 2019). Any distribution of this work must maintain attribution to the author(s), title of the work, publisher, and DOI